IEEE Access
Multidisciplinary | Rapid Review | Open Access Journal

Received March 19, 2020, accepted April 3, 2020, date of publication April 15, 2020, date of current version May 13, 2020.

Digital Object Identifier 10.1109/ACCESS.2020.2988000

Ultra-Wideband Differential Fed Hybrid Antenna With High-Cross Polarization Discrimination for Millimeter Wave Applications

MAGID ALZIDANI, (Graduate Student Member, IEEE), ISLAM AFIFI, (Graduate Student Member, IEEE), MUFTAH ASAADI, AND ABDEL-RAZIK SEBAK, (Life Fellow, IEEE)

Department of Electrical and Computer Engineering, Concordia University, Montreal, QC H4B 1R6, Canada

Corresponding author: Magid Alzidani (m_atiya@enccs.concordia.ca)

ABSTRACT A wideband differential fed patch antenna with high cross-polarization discrimination is proposed at mm-wave range. For the purpose of increasing antenna bandwidth, capacitive coupling technique is used. Also, the differential feeding is utilized to ensure broadside radiation and low cross-polarization. The designed antenna has an ultra-wide bandwidth of 55% around 30 GHz with $S_{11} \leq -10$ dB, and a peak gain of 8 dBi. The radiation pattern has a cross polarization level less than -20 dB over the operating frequency band. The differential feeding technique depends on equal power division and 180° phase difference for all the antenna bandwidth. Due to the wide bandwidth of the differential feeding antenna element, two designs of the feeding circuits (which include rat race and probe strip line transition) are used to cover the whole frequency band of the antenna. A gain enhancement has been achieved by adding a horn to the designed antenna with an efficient aperture efficiency. The designed antennas have fractional bandwidths of 28.73% (at center frequency 25.64GHz) and 26.3% (at the center frequency 32.2 GHz), for the lower and the upper bandwidths, respectively. An average gain of 14.5 dBi has been achieved for the frequency band from 21.8 GHz to 36.5 GHz. The antenna performance is verified through fabrication and measurement, where the simulated and measured results are in a good agreement.

INDEX TERMS Law cross polarization, differential feeding, wide band antenna, and hybrid antenna.

I. INTRODUCTION

Millimetre wave (mm-wave) band attracts a lot of attention in many applications such as wireless communications, imaging, and automotive radar. The mm-wave band has a wide bandwidth that can handle the growth of high data rate requirements [1]. Due to mm-wave characteristics such as high oxygen absorption and high free space propagation loss [2]–[4], a wideband high gain antenna is required. In addition, low cross polarization, and compact antenna is preferred for mm-wave applications. Millimeter wave high gain antennas can be used in back-haul communications, because it reduces radiation in undesired directions and boost the wireless channel link budget [5].Also, high gain mm-wave antenna could be used for automotive mm-wave sensors in order to improve driver safety [6], [7].

The associate editor coordinating the review of this manuscript and approving it for publication was Debdeep Sarkar.

Microstrip patch antenna is known by its unique and attractive properties such as low profile, light weight, ease of fabrication, and ability to be integrated with other devices easily. On the other hand, it suffers from a low impedance bandwidth and a low gain. Researchers have proposed many techniques to increase patch antenna impedance bandwidth. Patch antennas loaded by U, E or C slot shapes have a wideband [8], [9]. This is a well-established technique where the slots introduce other resonant frequencies that result in a wide bandwidth. However, the resulted surface current of patch's high order mode affects the antenna's directivity severely. Another approach to increase the antenna bandwidth is the usage of low permittivity substrate because charges in low permittivity material have high ability to generate flux in comparison with high permittivity material. High dielectric constant antenna is known for small area and narrow bandwidth in comparison with low permittivity antenna. In addition high permittivity material increases dielectric loss

[8], [10], [11]. In addition, increasing substrate thickness with low dielectric constant is used to boost antenna performance such as antenna bandwidth and radiation efficiency, however this method increases the cross-polarization level [8]. Another technique is the usage of differential feeding to have a wideband performance, and a symmetric radiation pattern which leads to low cross polarization [12], [13]. Also, a differential patch antenna is preferred in contrast with the single feeding antenna when integrating with differential devices. Moreover, cross polarization's radiation level of differential feeding antennas is much weaker than single feeding antenna whereas the co-polarized radiation level is matched [14].

Henceforth, the main focus in this paper is on designing a differential feeding antenna. Examples of previous works are presented here. In [15], Liu *et al.* presented a rectangular microstrip patch antenna fed using a differential technique in which the operating bandwidth is enhanced through the use of the TM_{10} and TM_{30} modes simultaneously. The TM_{10} mode is shifted up by using four short pins while the TM_{30} mode is shifted down by etching two long slots near the edges of this rectangular patch and becomes close to the shifted TM_{10} mode. However, this work provides only 13% impedance bandwidth, and an average gain of 6.4 dBi. Furthermore, the antenna is air suspended which makes it hard to be fabricated. Recently, Ahmed *et al.* [16] have used a differential feeding TM_{30} rectangular patch antenna loaded by two slots to achieve a high gain with low side lobe level. The two slots are etched in the out-of-phase region in order to reduce the out-of-phase surface current while keeping the in phase current. Also, they add new radiation elements in phase with the original antenna and hence enhance the gain. The antenna achieves a gain of 12.8 dB with side loop level of only −12.7 dB. Yet, the antenna has a bandwidth of 7% around 3GHz. In [17], differential fed patch antenna arrays are designed to operate at 13 GHz centre frequency. The first array is designed based on deploying the differential feeding to each element of the array while the second array design applies the differential scheme to the whole structure by feeding each pair of elements. The first array has an impedance bandwidth of 15.3% and 10.41 dBi gain with −17.5 dB cross polarization. The second array achieves a 12.32 dBi gain and a 12.8% impedance bandwidth with −17 dB cross polarization. The main idea of feeding pair of elements is to reduce the feeding network losses and hence increases the gain with small effect on the cross polarization level.

For increasing antenna bandwidth and gain simultaneously, the hybrid configuration technique is used. Generally hybrid antenna consists of an active element, parasitic element, and a metallic fence. In this technique, both the active element, and the parasitic element have a different resonance frequency that are slightly apart from each other, resulting in a wide bandwidth. While the metallic fence (horn antenna) is incorporated to increase the antenna gain [18]–[21]. This technique has the advantage of having a high gain with low profile antennas compared to conventional horn antennas. In [18], hybrid dielectric resonator antenna (HDRA) is designed in which a circular patch antenna is used to excite a ring dielectric resonator antenna and a conical cavity is also incorporated to improve the antenna gain. However, the designed work achieved a gain of about 16.5 dBi with a −10 dB matching bandwidth in the frequency band from 57 to 64 GHz. Elboushi and Sebak [19] designed a hybrid antenna by using a surface mounted conical horn with a circular patch antenna in order to enhance the gain. They achieved a 12 dBi gain and 10% bandwidth around 31 GHz. However, similar to [18] and [19], it has a narrow bandwidth that is less than 12%. In [20], a Fabry–Perot resonance antenna with two layer stacked superstrate is used to feed a conical horn antenna operating at a center frequency of 12 GHz. The design achieved 19.1 dBi and 26%, peak gain and 3-dB gain bandwidth, respectively. However the antenna's aperture efficiency is 27%, which is considered low. Another hybrid configuration consists of a cross dielectric resonator antenna excited by a patch antenna and surrounded by a rectangular horn is presented by Nasimuddin *et al.* in [21]. However, a 21.3% impedance bandwidth, and a gain better than 9 dBi at a centre frequency of 6.8 GHz was achieved. Patch antenna can be fed using gap coupling strip in order to enhance antenna bandwidth. In this technique coaxial probe feeds a short strip, which is used to excite the patch. The probe introduces an inductance, the gap between the patch and the strip introduce a capacitance, and the strip introduces radiation resistance. The three elements produce extra new resonance circuit. As a result, the patch and the coupling gap circuit create a dual resonance frequencies. Moreover, coupling techniques allow the patch to be excited only in a single mode operation, in which the patch and the resonator are resonating, and suppressing other harmonics [22].

The aim of this paper is to design a wideband broadside low cross polarization antenna. Capacitive feeding technique is used to enhance antenna bandwidth where two resonance frequencies are generated. However the antenna radiation pattern is not extreme in the broadside direction which has a negative impact if the antenna arranged in an array form. In order to deal with this issue, the differential and gap coupling capacitive techniques are used for cross polarization discrimination and bandwidth enhancement. The rectangular strips are used in order to couple the exciting signal to the radiated patch. Then, hybrid technique is employed for gain incrimination.

The paper is organized as follows: In section II, the antenna theory is discussed, followed by antenna design including single capacitive coupling feeding technique, differential feeding antenna design, and the hybrid antenna are presented in section III. Section IV shows the experimental and the simulation results of the proposed antennas. The article ends with a conclusion in section V.

II. ANTENNA THEORY

Exploiting of differential feeding features is related to the understanding of the antenna field distribution. Patch

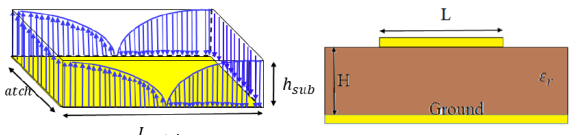

FIGURE 1. Electric field distribution of patch antenna.

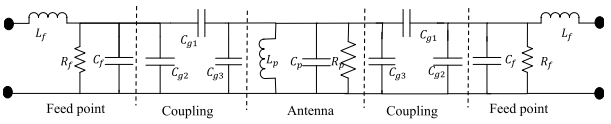

FIGURE 2. Capacitive and differential feeding patch antenna equivalent circuit.

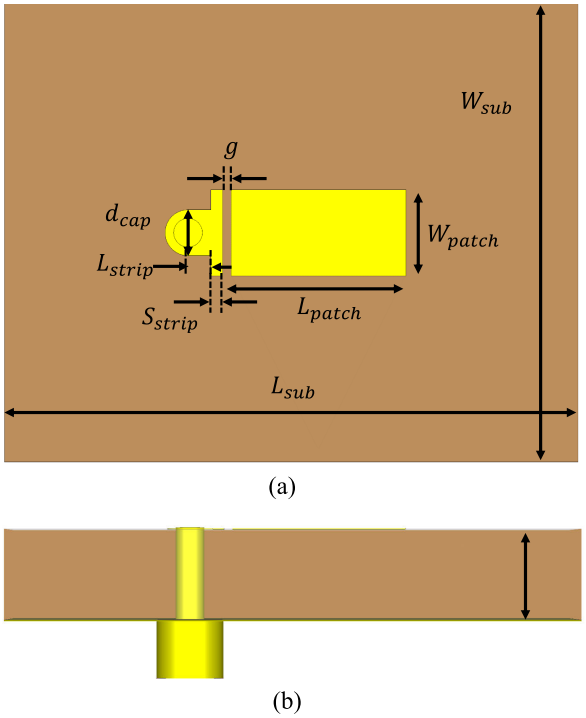

FIGURE 3. Configuration of the designed capacitive feeding patch antenna. (a) Top view. (b) Side view.

antenna's E-field lines distribution can be expressed using cavity model (TM_{100} mode) with perfect magnetic conductor (PMC) walls surrounding the antenna, while excluding fringing field's effect [8]. The antenna radiation pattern can be expressed by two radiating slots separated by the patch length(L). Each slot radiates as the same field as a magnetic dipole [12]. Accordingly, the patch field distribution has a cosine shape and uniform shape along the antenna length and width, respectively as shown in Fig. 1.

The desired field vector component is called co-polarized field and the field vector that is normal to it is called cross-polarized field. The cross-polarization is associated with the fields on the none-radiating edges of the patch.

In case of single feed antenna, the field amplitude is not symmetry along the antenna length and hence the cross polarization field's intensity becomes weak as moving away from the feeding point which results in non-zero cross-polarization field in the broadside direction. Accordingly, cancellation of this asymmetry is the key factor for cross-polarization suppression. There is one known way to cancel this difference and it is done through feeding the antenna at the two ends by the same signal with 180° phase shift. Due to equalization of vector field intensity at both ends of the patch antenna, symmetric radiation pattern is generated and cross-polarization level is suppressed. Single layer patch antenna is known by narrow bandwidth, so bandwidth incrimination brings a challenging task in the design of patch antenna. Since a patch antenna is considered as a *RLC* resonance circuit, introducing another resonance frequency enhances antenna bandwidth as in [23], [24]. For this purpose, a resonator consists of a probe with a cap and a rectangular strip is employed. The patch is excited in capacitive way through the resonator, in which coupling gap width is adjusted to make the two resonance frequencies close to each other in order to have a wide matching bandwidth. The equivalent circuit model of the proposed antenna is shown in Fig.2. The patch antenna is represented by a resonator of R_p L_p C_p, the feeding probes at both sides of the patch antenna are represented by C_f R_f L_f, and the coupling gaps are represented by a π network C_{g1} C_{g2} C_{g3} at each end. First, the feeding point, L_f represents the probe inductance, C_f represents the probe cap capacitance, and the cap radiation loss is represented by R_f. Second, the capacitive coupling, C_{g1} represents the edge capacitance between the patch and the rectangular strip ends, C_{g2} represents the strip edge capacitance, and C_{g3} represents the patch edge capacitance.

III. ANTENNA DESIGN

A. SINGLE FEEDING ANTENNA DESIGN

This work presents the design of a rectangular microstrip patch antenna fed by capacitive coupling. The antenna layout is illustrated in Fig. 3. The microstrip patch antenna is placed on a dielectric substrate (Rogers 5880, $\epsilon_r = 2.2$ and thickness = 1.575 mm). The capacitive coupling method is used to enhance the antenna bandwidth, in which a rectangular strip (resonators) is employed to generate another resonance frequency. The rectangular strip is placed at a coupling gap distance (g) from one of the patch radiating edges, and connected directly to the coaxial feeding probe. The probe position of tradition patch antenna must be adjusted in order to find the proper feeding point for good matching. However, in this work, radiation pattern is not sensitive to probe position. The antenna is designed and its parameter dimensions are shown in Table 1.

The computer simulation technology (CST) software package is used to simulate the proposed antenna. The designed antenna reflection coefficient and the gain are shown in Fig. 4. The simulated matching bandwidth is 56.8% at 30 GHz which

TABLE 1. Capacitive feeding patch antenna geometrical parameters.

Parameter	W_{patch}	L_{patch}	W_{sub}	L_{sub}	S_{strip}
Value (mm)	1.5	6.1	10	8	0.15
Parameter	L_{strip}	g	h_{sub}	d_{coax}	d_{coax2}
Value (mm)	0.5	0.15	1.575	0.5	1.15

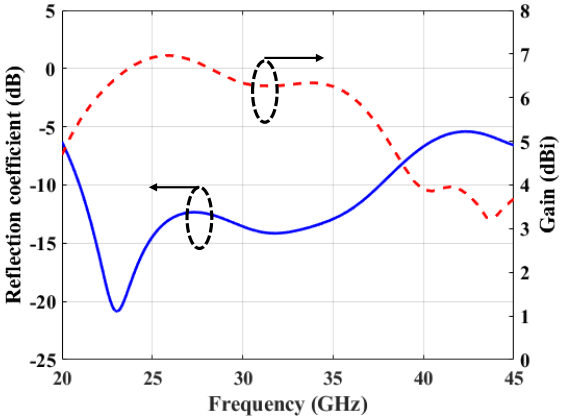

FIGURE 4. Patch antenna reflection coefficient and gain.

is wider than regular patch antenna. In general, low gain is one of the patch antenna drawbacks, the simulated realized gain is 6.5 dBi at the center frequency. Fig. 5 shows the co-polar and the cross-polar radiation patterns at ($\phi = 45°$) for four different frequencies using Ludwig III definition. The 45° cut has been chosen because it shows all the radiation pattern information and according to the Body of Revolution (BOR) theory, the peak level of cross-polarization is at 45° [25]. Therefor, the whole radiation pattern of the desired antenna can be reconstructed from 45° cut in E and H plane. Fig.5 shows minimum cross-polarization of about −8 dB. The radiation pattern of the antenna is asymmetry in the E-plane due to the drawback of the single feeding. Furthermore, the antenna main lobe is tilted with frequency ([−14° + 7°]); this tilt should be taken into account in case of designing an array antenna. Fig .6. shows the antenna 3D radiation pattern at 28GHz, that clarify the tiled beam. The working principle can be explained by the electric field distribution shown in Fig. 7. The solid arrows show that, the synthetic electric vector on the coupling edge is along x-direction and, hence, x-polarization is introduced. The electric field density of capacitive feed antenna is concentrated more at the feeding edge in comparison to the far end. This is the drawback of using single feed antenna, which cause beam tilting in addition to high cross-polarization.

The typical goal of this parametric study is to show the effect of specific parameters of the designed antenna on the gain and the impedance matching bandwidth (s11<10dB). The selected parameters that related to the capacitive feeding part are L_{strip}, S_{strip}, and g. The effect of L_{strip} is shown in Fig. 8 where the gain and the matching are improved at high frequencies as L_{strip} decreases. Fig. 9 shows the effect

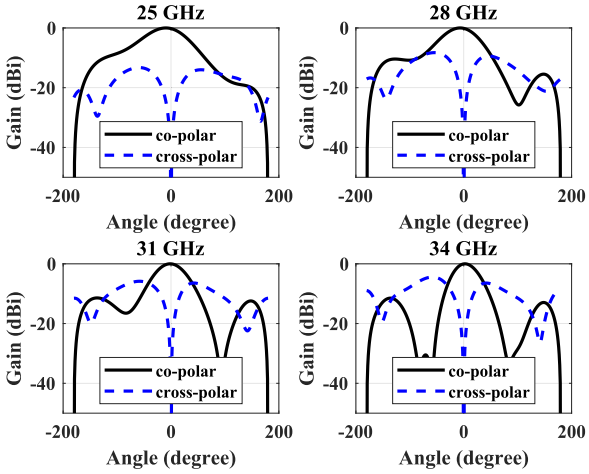

FIGURE 5. Co and cross polar radiation pattern ($\phi = 45°$).

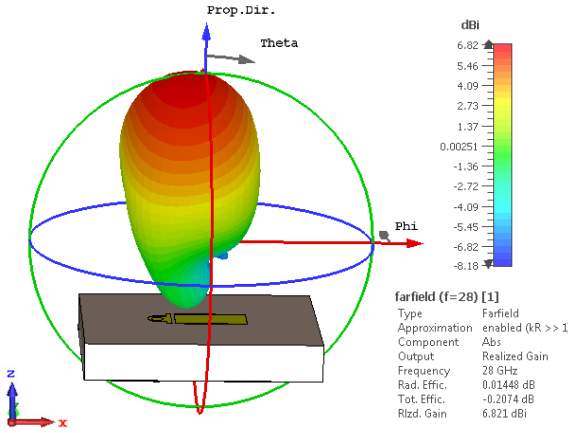

FIGURE 6. 3D radiation pattren of single feed antenna ($f = 28$ *GHz*).

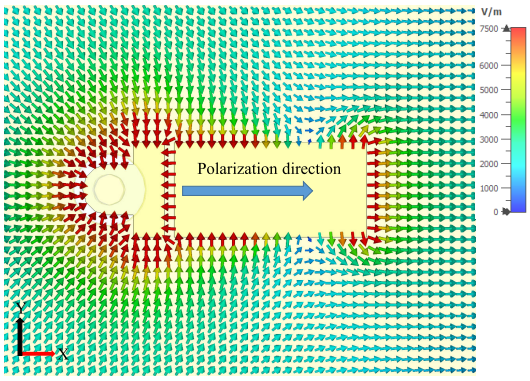

FIGURE 7. E-field distribution of single feed patch antenna.

of S_{strip}, where there is very small effect on the antenna gain. However, the bandwidth is inverse proportional to the S_{strip} length. The effect of S_{strip} and L_{strip} referred to that, increasing S_{strip} or L_{strip} increases the capacitance and hence shift the resonance frequency of the feeding part toward the patch resonance and decrease the overall bandwidth. Fig. 10

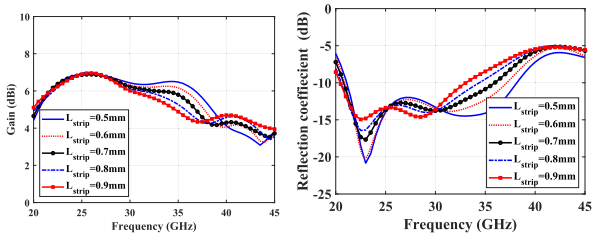

FIGURE 8. Parametric study of the effect of L_{strip} on (a) antenna gain (b) antenna matching bandwidth.

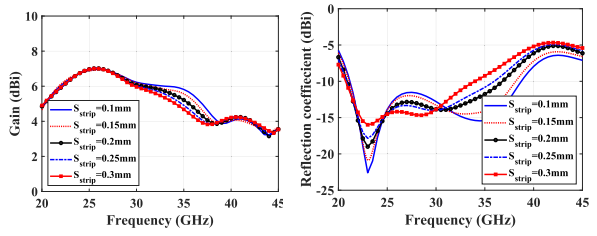

FIGURE 9. Parametric study of the effect of S_{strip} on (a) antenna gain (b) antenna matching bandwidth.

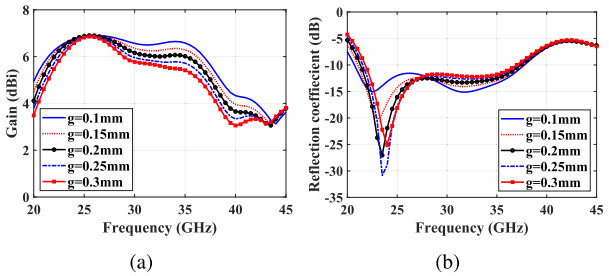

FIGURE 10. Parametric study of coupling gap distance on (a) antenna gain (b) antenna matching bandwidth.

shows the effect of the coupling gap. At low frequency band, the gap coupling does not affect the antenna gain. However, a small shift in the resonance frequency of the patch is observed toward the lower frequency band when decreasing the gap distance. While, at high frequencies, the antenna gain and bandwidth increases when the gap coupling decreases.

B. DIFFERENTIAL FEEDING ANTENNA DESIGN

In this subsection, the patch antenna is excited deferentially at both radiating ends. This technique is used to overcome the tilting in the radiation pattern and the high cross-polarization level presented in the previous design. The differential feeding is achieved by adding another capacitive feeding strip at the other end of the patch antenna, physical symmetry of the feeding points' location should be extremely considered. The antenna is designed on the same substrate and its layout is shown in Fig. 11, and its dimensions are presented in Table 2. Fig. 12. shows the antenna simulated reflection coefficient and gain, in which a wide bandwidth is achieved (more than

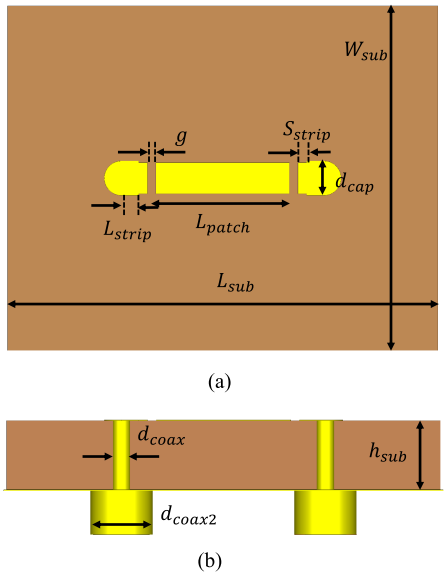

FIGURE 11. Differential feeding antenna. (a) Top view (b) Side view.

TABLE 2. Optimized geometrical parameters for the differential feeding patch antenna.

Parameter	W_{patch}	L_{patch}	W_{sub}	L_{sub}	S_{strip}
Value (mm)	0.72	3.1	10	8	0.2
Parameter	L_{strip}	g	h_{sub}	d_{coax}	d_{coax2}
Value (mm)	0.5	0.15	1.575	0.4	0.4

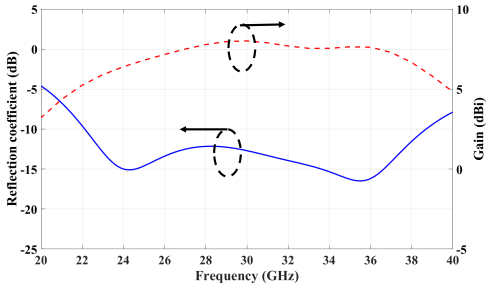

FIGURE 12. Capacitive differential feeding patch antenna reflection coefficient and gain.

55% at 30 GHz). Moreover, the antenna gain is increased to reach 8 dBi instead of 6.5 dBi for the single feeding antenna. Fig. 13. shows the 3D radiation pattren of the differential feeding antenna, which is symmetrical more than the single feeding antenna.

The antenna E-field distribution is presented in Fig.14. The solid arrows show that the synthetic electric vector on the coupling edges is along the x-direction and co-polarization is introduced. The electric field's distribution density are equal in value and symmetrical with respect to both xz and yz-planes. The excitation through both ends of the patch antenna differentially generates two different voltage pols (+v and –v). The pols at the coupling gaps generate symmetric electric fields in the same direction, moreover the electric field distribution along the x-axis are uniform. The fields

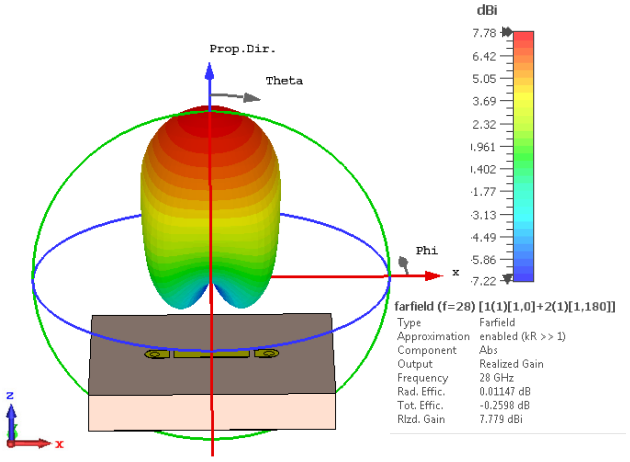

FIGURE 13. 3D radiation pattern of differential feeding antenna at ($f = 32$ *GHz*).

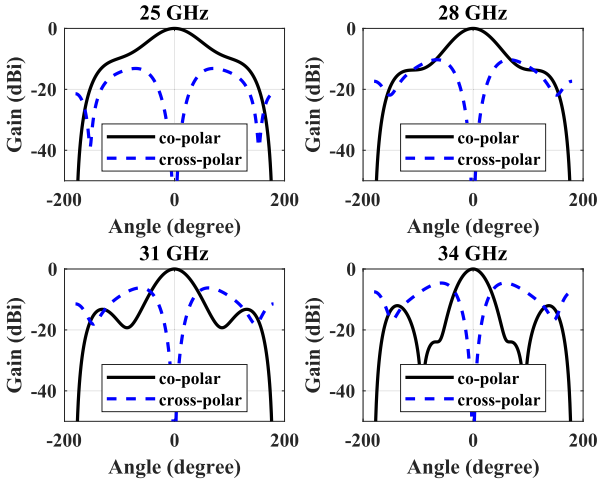

FIGURE 15. Ludwig III Co and cross polar radiation pattern of differential feeding antenna ($\phi = 45°$).

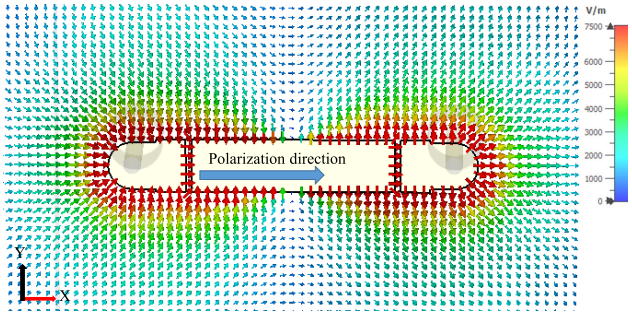

FIGURE 14. E-field distribution of differential feeding antenna.

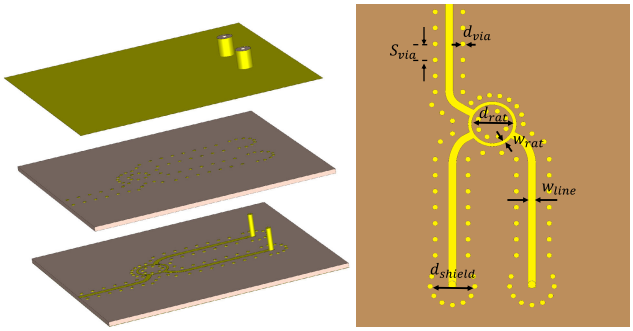

FIGURE 16. Rate race and transition line configuration.

orthogonal to yz-plane construct the co-polar radiation patter, whereas the fields orthogonal to xz-plane produce the cross-polar radiation pattern; these fields are opposite in direction, so the resulted cross-polar in the far field region is zero along yz-plane.

Fig.15 shows Ludwig III Co and cross polar radiation patterns of the differential feeding antenna ($\phi = 45°$) for four frequencies, which covers the whole operating band. The differential feeding technique has a positive impact on the radiation pattern compared to the single antenna feeding, in which Fig.15 indicates a high level of symmetry of the radiation pattern and lower cross-polarization level compared to the single feed antenna as well. Moreover the radiation pattern is broadside with no tilting angle, while the radiation pattern of single feed antenna is tilted about 14°. In terms of antenna realized gain, the differential feeding antennas has a bit higher gain.

C. DIFFERENTIAL FEEDING DESIGN

The feeding circuit is implemented by employing a strip rat race coupler, which is used to feed two probes (+v and-v) by an equal amplitude and out-of-phase signals. The transition from the strip line to the antenna probe and the strip line rat race coupler are designed as shown in Fig.16. This feeding circuit is considered as the candidate choice because it is easily fabricated, no radiation loss, and inexpensive compared with conventional waveguide. The transition circuit is shielded using vias around the probe and the strip line to prevent leakage. The shielding technique is designed based on two factors, the via radius d_{via} and the distance between the two adjacent vias s_{via}, similar to the substrate integrated waveguide technique [26], [27].

$$d_{via} \leq \frac{\lambda_g}{5} \quad (1)$$

$$s_{via} \leq 2d_{via} \quad (2)$$

The isolated port of the rat race coupler, usually, is terminated with a matched load. Basically, the matched load is a 50Ω lumped element which is not easy to fabricate in mm-wave band. In the designed coupler, the isolation level is better than 15dB, henceforth, this port is removed without affecting the rat race behavior. The rat race coupler has almost equal power division in a limited bandwidth. In order to have a good differential feeding, this limitation forces us to divide the antenna operating bandwidth into two bands, which are (22 to 30) GHz and (30 to 38) GHz. Therefore, there is two values for the radius of the rat race depending on the operating

TABLE 3. Optimized geometrical parameters for the rat race and the transition component.

Parameter	d_{via}	S_{via}	d_{shield}	d_{rat}	w_{rat}	w_{line}
Value (mm)	0.15	0.3	1.4	2.4-3.2	0.2	0.45

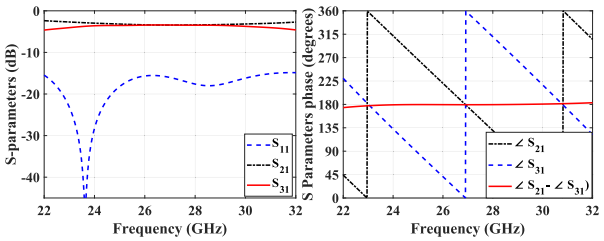

(a) (b)

FIGURE 17. Rat race and transition circuit for the lower band (a) S-parameters (b) phase response.

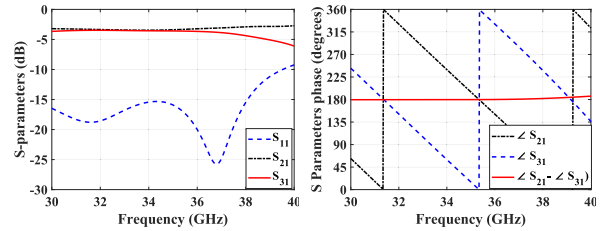

(a) (b)

FIGURE 18. Rat race and transition circuit for the upper band (a) S-parameters (b) phase response.

frequency. A radius of 1.6 mm is used for the lower frequency band and a radius of 1.2 mm is used for the higher frequency band. Dimensions of the rat race and the transition part are presented in Table 3. The simulated reflection coefficient amplitude and phase of the feeding circuit including the rat race and the transition are shown in Fig. 17 and Fig.18 for two operating bands. The figures indicate that $S_{11} \leq -15$ dB for the whole operating band of the antenna, and equal power division with 180°phase difference.

D. HYBRID ANTENNA

The proposed wideband antenna can be used to achieve a high data rate at mm-wave band. However, due to mm-wave characteristics, a high gain antenna is also required. One way to increase antenna gain is by employing a horn antenna on top of the designed antenna. The proposed horn antenna is designed based on the equations in [28], where the phase error coefficients: t, and s values are chosen as 0.375 and 0.25, respectively, for the optimum horn design. The following equations shows the t and s are function of the antenna geometric parameters A, B, R_1, and R_2.

$$t = \frac{A^2}{8\lambda_0 R_1} \quad s = \frac{B^2}{8\lambda_0 R_2} \tag{3}$$

where A and B are the dimensions of the horn antenna aperture and R_1 and R_2 are the dimensions from the horn aperture

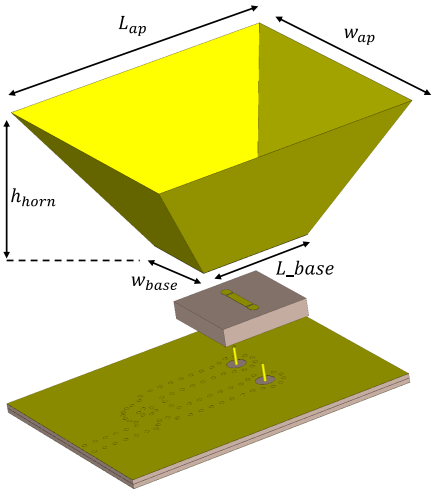

FIGURE 19. Hybrid antenna configuration.

TABLE 4. Horn antenna parameters.

Parameter	L_{ap}	w_{ap}	h_{horn}	w_{base}	l_{base}
Value (mm) Ant. 1	23.95	23.95	11.37	8	11.3
Value (mm) Ant. 2	23.95	23.95	12	8	12

to the phase center in the E and H-planes. The antenna gain is determined by the following equation.

$$G = \varepsilon_{ap} \frac{4\pi}{\lambda_0^2} AB \tag{4}$$

where the aperture efficiency ε_{ap} is taken as 51 %. Finally we get the following design equation for and optimum horn antenna.

$$\frac{3}{2}\left(\frac{G\lambda_0^2}{4\pi\,\varepsilon_{ap}}\right)^2 - \frac{3G\lambda_0^2}{8\pi\,\varepsilon_{ap}} Ab = A^4 - aA^3 \tag{5}$$

The horn design parameters are first calculated based on having a gain of 15 dBi at the center frequency and the values of the inner feeding aperture is $8 \times 8\ mm^2$ (the patch antenna size). Since the inner feeding aperture controls the designed horn antenna, the antenna parameters have been optimized to get good impedance matching and high gain. The resulted hybrid antenna configuration can be seen in Fig.19, and it is associated dimensions are listed in Table 4.

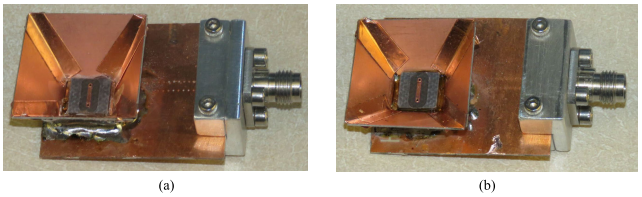

(a) (b)

FIGURE 20. Prototype antennas at frequency range (a) f = (21.8-29)GHz, (b) f = (29-36.5)GHz.

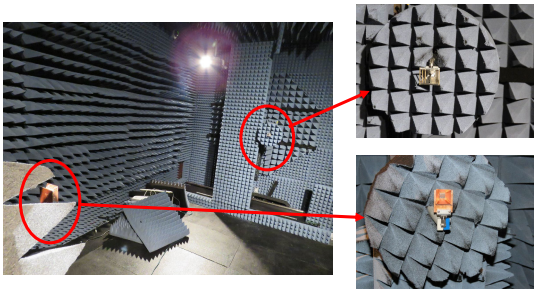

FIGURE 21. Antenna radiation pattren measurements setup.

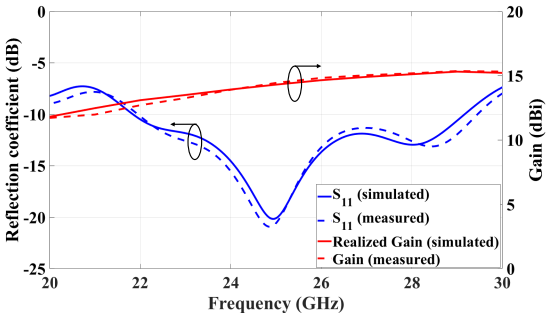

FIGURE 22. Hybrid antenna reflection coefficient and gain.

IV. RESULTS AND DISCUSSION

Prototype of the proposed antennas are fabricated using PCB multi-layer technology, while the horn part has been made using four pieces of coppers and assembled by conducting tape then soldered together. Two prototypes for the frequency range (21.8-29.3) GHz and (28-36.5) GHz are shown in Fig. 20. The programmer network analyzer (PNA N52271A) is used to measure the reflection coefficients, and the Anechoic chamber is used to measure antenna's radiation pattern and gain.

Fig. 21. shows the radiation pattern measurements set up in the chamber. The measured S_{11} and gain are shown in Fig. 22. and Fig. 23 along with the simulated results for the frequency range (21.8-29.3)GHz and (28-36.5)GHz, respectively. The maximum realized gain of the first design (21.8-29.3 GHz) is 15.2 dBi, and the ($S_{11} \leq -10$ dB) is 28.73%. The

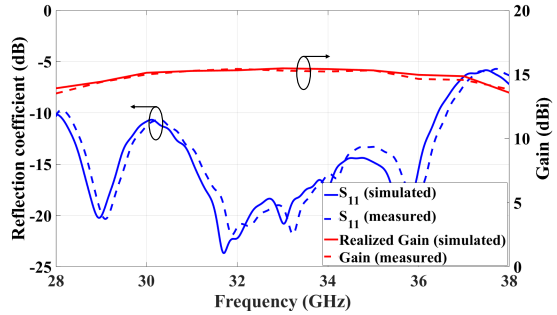

FIGURE 23. Hybrid antenna reflection coefficient and gain.

TABLE 5. Table of comparison.

Refrence No	f (GHz)	Gain (dBi)	BW(%)	Aperture efficiency(%)
[18]	62	16.5	11.23	47
[19]	31	12	10	89
[20]	12	19.1	26	49.3
[21]	6.8	9	21.3	59
Proposed(1)	25.6	15	28.7	60
Proposed (2)	32.2	15	26.3	38.1

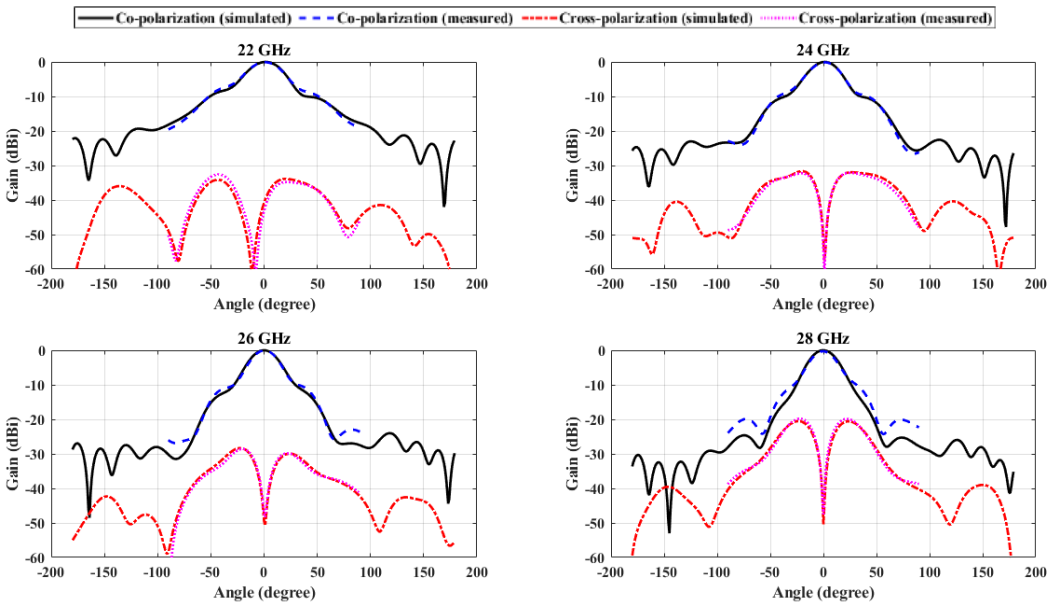

FIGURE 24. Co and cross-polar E-plane radiation pattern of hybrid antenna at frequency range (21.8-29)GHz.

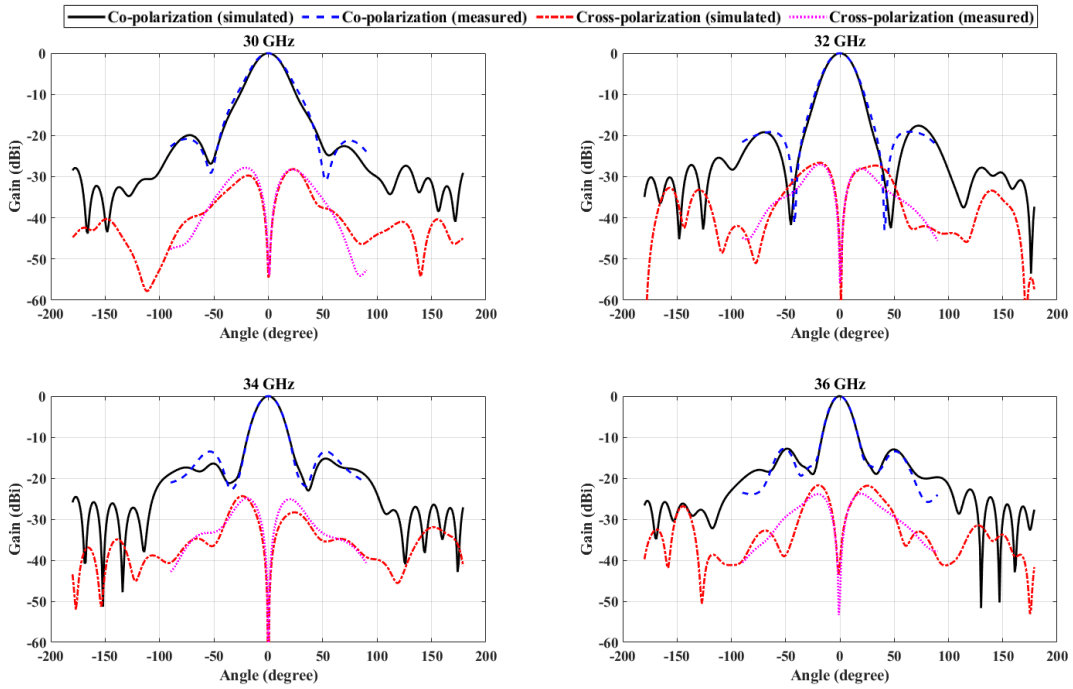

FIGURE 25. Co and cross-polar E-plane radiation pattern of hybrid antenna at frequency range (29-36.5)GHz.

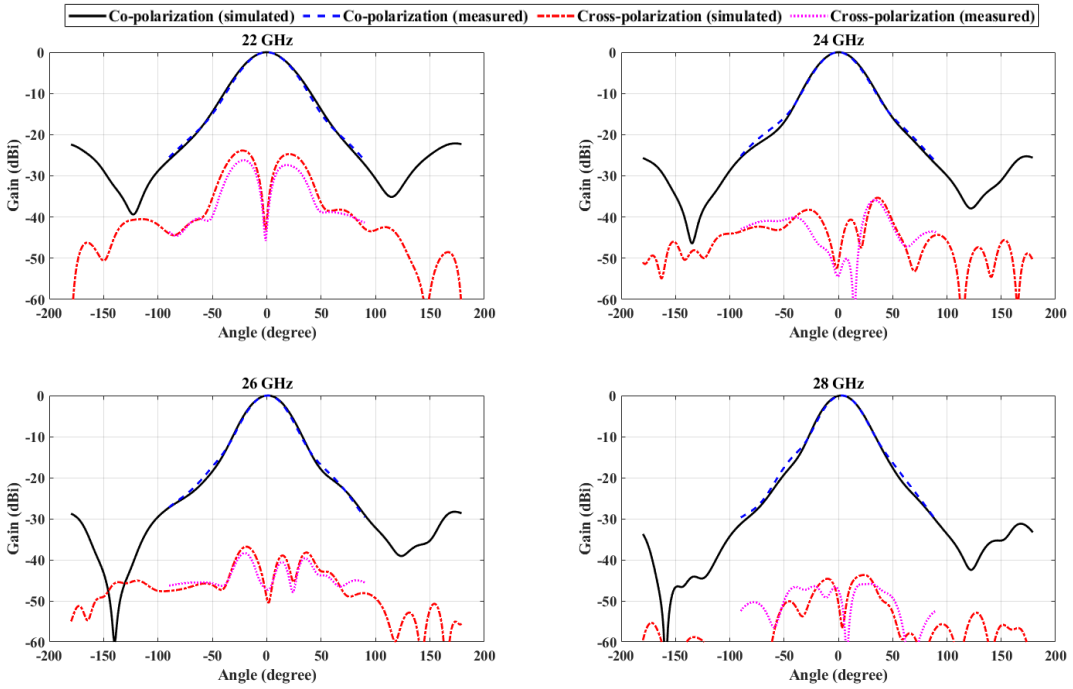

FIGURE 26. Co and cross-polar H-plane radiation pattern of hybrid antenna at frequency range (21.8-29)GHz.

second design (29-36.5 GHz), has a maximum realized gain of 15.5 dBi and return loss bandwidth is 26.3%.

A comparison among related reported antennas and this work is divided into two themes. Theme I, comparing the differential antenna with works in [15]–[17], the differential antenna has wider bandwidth and acceptable gain. Moreover the designed antenna in [15] is air suspended which made it hard to fabricate.

In theme II, a comparison in terms of hybrid antenna is listed in Table 5. Hybrid antenna techniques has been used

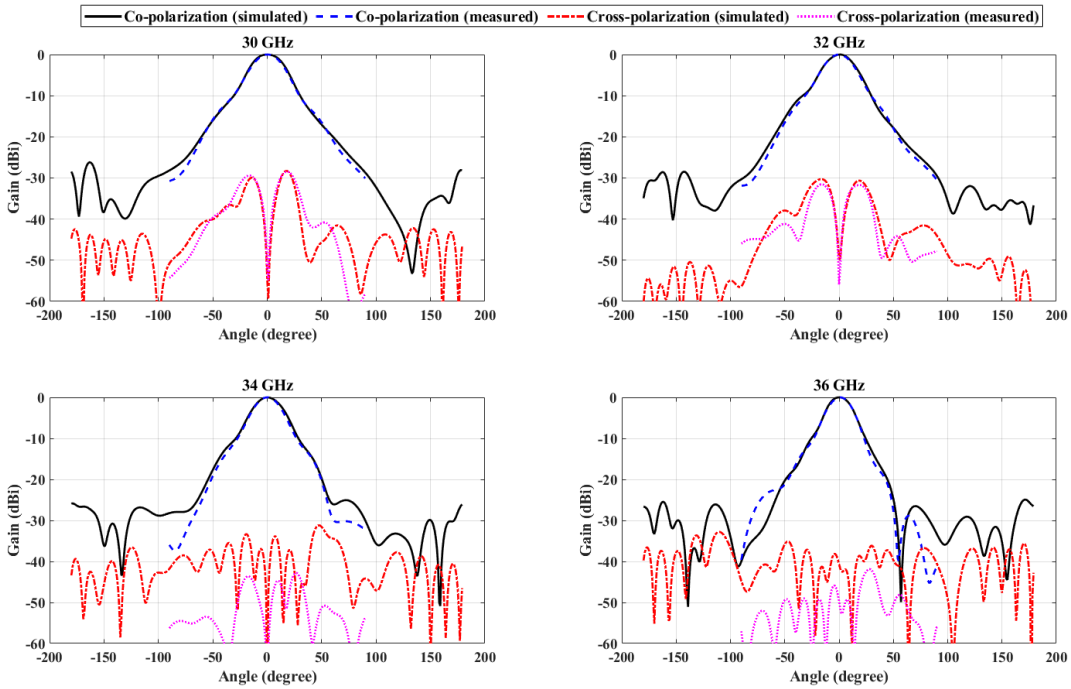

FIGURE 27. Co and cross-polar H-plane radiation pattern of hybrid antenna at frequency range (29-36.5)GHz.

for increasing antenna gain. This work has some advantages compared to other designed antennas in which capacitive and differential feeding techniques are used. The differential feeding antenna provided low cross-polarization, and low side lobe level. Moreover, the matching bandwidth has been enhanced compared to the reported works. Work in [20] is two layers stacked superstrates combined with horn antenna to boost the antenna gain, which make it bulky. In [21] a patch antenna excites a dielectric resonator to feed the horn antenna is used. However, the resulted antenna gain is just 9 dBi. Fig. 24 and Fig.25 show the simulated, and measured co-polar and cross-polar radiation patterns of the hybrid antenna in the E-plane, at the frequency ranges (21.8-29)GHz and (29-36.5)GHz, respectively. While, Fig. 26 and Fig. 27 present the simulated, and measured H-plane radiation pattern of the hybrid antenna. The measured results are obtained but it covers just 180° because of measurements facilities limitations. The cross-polar radiation is very weak that indicates the positive impact of the differential feeding technique. The simulated and the experimented results are in a good agreement, in which the highest cross polarization level is −30 dB. The slight deviation between the measured and simulated results may come from the change of the permittivity at high frequencies, as the used material permittivity is given at 10 GHz. Also, the fabrication accuracy could cause some errors.

V. CONCLUSION

In this paper, the differential feeding and capacitive feeding techniques are implemented on the patch antenna design. The patch antenna is fed using capacitive technique to increase the antenna bandwidth, and also the differential techniques is used to decrease the cross polarization level. Rat race coupler and coaxial to strip line transition are designed as well for feeding purpose. The antenna simulated bandwidth is 55% at 30 GHz. Finally, a horn antenna is employed on the top to have a high gain antenna that overcome the high path losses at mm-wave range. The designed hybird antenna achieves a total bandwidth of 50.5% and maximum gain of 15.5 dBi. Due to the wideband of the single antenna element, the antenna can be used for indoor wireless communication and medical imaging. The Proposed hybrid antenna offers wide bandwidth and sufficient gain, so it can be used for many applications such as automotive radar and outdoor wireless communication.

REFERENCES

[1] S. Lian, "Evolution from 3G to 4G and beyond (5G)," *Int. J. Eng. Sci. Comput.*, vol. 6, no. 4, pp. 4250–4251, 2016.
[2] T. S. Rappaport, S. Sun, R. Mayzus, H. Zhao, Y. Azar, K. Wang, G. N. Wong, J. K. Schulz, M. Samimi, and F. Gutierrez, "Millimeter wave mobile communications for 5G cellular: It will work!" *IEEE Access*, vol. 1, pp. 335–349, 2013.
[3] E. Dahlman, S. Parkvall, D. Astely, and H. Tullberg, "Advanced antenna solutions for 5G wireless access," in *Proc. 48th Asilomar Conf. Signals, Syst. Comput.*, Nov. 2014, pp. 810–814.
[4] Z. Qingling and J. Li, "Rain attenuation in millimeter wave ranges," in *Proc. 7th Int. Symp. Antennas, Propag. EM Theory*, Oct. 2006, pp. 609–612.
[5] H. Schantz, *The Art and Science of Ultra-Wideband Antennas*. Norwood, MA, USA: Artech House, 2005.
[6] R. Rehammar, Z. Liang, and B. Billade, "Design of a sensor agnostic FMCW-compatible transponder for automotive applications," in *Proc. IEEE Conf. Antenna Meas. Appl. (CAMA)*, Västerås, Sweden, Sep. 2018, pp. 1–4.

[7] M. G. N. Alsath, L. Lawrance, and M. Kanagasabai, "Bandwidth-enhanced grid array antenna for UWB automotive radar sensors," *IEEE Trans. Antennas Propag.*, vol. 63, no. 11, pp. 5215–5219, Nov. 2015.

[8] W. L. Stutzman and G. A. Thiele, "Antenna theory and design," *IEEE Antennas Propag. Soc. Newslett.*, 1981.

[9] R. Chair, C.-L. Mak, K.-F. Lee, K.-M. Luk, and A. A. Kishk, "Miniature wide-band half U-slot and half E-shaped patch antennas," *IEEE Trans. Antennas Propag.*, vol. 53, no. 8, pp. 2645–2652, Aug. 2005.

[10] L. C. Paul, "The effect of changing substrate material and thickness on the performance of inset feed microstrip patch antenna," *Amer. J. Netw. Commun.*, vol. 4, no. 3, p. 54, 2015.

[11] P. Katehi and N. Alexopoulos, "On the effect of substrate thickness and permittivity on printed circuit dipole properties," *IEEE Trans. Antennas Propag.*, vol. 31, no. 1, pp. 34–39, Jan. 1983.

[12] S. Bhardwaj and Y. Rahmat-Samii, "Revisiting the generation of cross-polarization in rectangular patch antennas: A near-field approach," *IEEE Antennas Propag. Mag.*, vol. 56, no. 1, pp. 14–38, Feb. 2014.

[13] Z. Tong, A. Stelzer, and W. Menzel, "Improved expressions for calculating the impedance of differential feed rectangular microstrip patch antennas," *IEEE Microw. Wireless Compon. Lett.*, vol. 22, no. 9, pp. 441–443, Sep. 2012.

[14] Y. P. Zhang and J. J. Wang, "Theory and analysis of differentially-driven microstrip antennas," *IEEE Trans. Antennas Propag.*, vol. 54, no. 4, pp. 1092–1099, Apr. 2006.

[15] N. W. Liu, L. Zhu, and W. W. Choi, "A differential-fed microstrip patch antenna with bandwidth enhancement under operation of TM_{10} and TM_{30} modes," *IEEE Trans. Antennas Propag.*, vol. 65, no. 4, pp. 1607–1614, Feb. 2017.

[16] Z. Ahmed, M. M. Ahmed, and M. B. Ihsan, "A novel differential fed high gain patch antenna using resonant slot loading," *Radioengineering*, vol. 27, no. 3, pp. 662–670, Sep. 2018.

[17] H. Jin, K.-S. Chin, W. Che, C.-C. Chang, H.-J. Li, and Q. Xue, "Differential-fed patch antenna arrays with low cross polarization and wide bandwidths," *IEEE Antennas Wireless Propag. Lett.*, vol. 13, pp. 1069–1072, 2014.

[18] E. Erfani, T. Denidni, S. Tatu, and M. Niroo-Jazi, "A broadband and high gain millimeter-wave hybrid dielectric resonator antenna," in *Proc. 17th Int. Symp. Antenna Technol. Appl. Electromagn. (ANTEM)*, Jul. 2016, pp. 1–2.

[19] A. Elboushi and A. Sebak, "High-gain hybrid microstrip/conical horn antenna for MMW applications," *IEEE Antennas Wireless Propag. Lett.*, vol. 11, pp. 129–132, 2012.

[20] Y. Ge, Z. Sun, Z. Chen, and Y.-Y. Chen, "A high-gain wideband low-profile Fabry–Perot resonator antenna with a conical short horn," *IEEE Antennas Wireless Propag. Lett.*, vol. 15, pp. 1889–1892, 2016.

[21] K. P. Esselle, "A low-profile compact microwave antenna with high gain and wide bandwidth," *IEEE Trans. Antennas Propag.*, vol. 55, no. 6, pp. 1880–1883, Jun. 2007.

[22] L. Inclan-Sanchez, J.-L. Vazquez-Roy, and E. Rajo-Iglesias, "Proximity coupled microstrip patch antenna with reduced harmonic radiation," *IEEE Trans. Antennas Propag.*, vol. 57, no. 1, pp. 27–32, Jan. 2009.

[23] J.-D. Zhang, L. Zhu, Q.-S. Wu, N.-W. Liu, and W. Wu, "A compact microstrip-fed patch antenna with enhanced bandwidth and harmonic suppression," *IEEE Trans. Antennas Propag.*, vol. 64, no. 12, pp. 5030–5037, Dec. 2016.

[24] V. G. Kasabegoudar and K. J. Vinoy, "Coplanar capacitively coupled probe fed microstrip antennas for wideband applications," *IEEE Trans. Antennas Propag.*, vol. 58, no. 10, pp. 3131–3138, Oct. 2010.

[25] J. M. Gil, J. Monge, J. Rubio, and J. Zapata, "A CAD-oriented method to analyze and design radiating structures based on bodies of revolution by using finite elements and generalized scattering matrix," *IEEE Trans. Antennas Propag.*, vol. 54, no. 3, pp. 899–907, Mar. 2006.

[26] F. Xu and K. Wu, "Guided-wave and leakage characteristics of substrate integrated waveguide," *IEEE Trans. Microw. Theory Techn.*, vol. 53, no. 1, pp. 66–73, Jan. 2005.

[27] K. Phalak and A. Sebak, "Surface integrated waveguide based triangular cavity backed t slot planar antenna at 60 GHz," in *Proc. IEEE Antennas Propag. Soc. Int. Symp. (APSURSI)*, Memphis, TN, USA, Jul. 2014, pp. 1495–1496.

[28] W. L. Stutzman and G. A. Thiele, *Antenna Theory and Design*, vol. 53. Hoboken, NJ, USA: Wiley, 1998.

MAGID ALZIDANI (Graduate Student Member, IEEE) received the B.Sc. degree in communication engineering and the M.Sc. degree in personal mobile and communication engineering from the College of Electronic Technology, Beni Walid, in 1994, and the M.Sc. degree from Bradford University, Bradford, U.K., in 2004. He is currently pursuing the Ph.D. degree in electrical and computer engineering with Concordia University, Montreal, QC, Canada. He was a Teaching and a Research Assistant with the Electric Department, from 2005 to 2014. His research interest includes millimeter-wave microwave components and antennas.

ISLAM AFIFI (Graduate Student Member, IEEE) received the B.Sc. degree in electronics and communication engineering and the M.Sc. degree in engineering physics from Cairo University, Cairo, Egypt, in 2009 and 2014, respectively. He is currently pursuing the Ph.D. degree in electrical and computer engineering with Concordia University, Montreal, QC, Canada. He was a Teaching and a Research Assistant with the Engineering Mathematics and Physics Department, from 2009 to 2014, and a Senior Teaching Assistant, from 2014 to 2016. His research interest includes millimeter-wave microwave components and antennas.

MUFTAH ASAADI received the B.Sc. degree in electronics and communications engineering from the College of Electronic Technology, Baniwaleed, Libya, in 2001, the M.Sc. degree in electrical and computer engineering from Libyan Academy, Libya, in 2009, and the Ph.D. degree in electrical and computer engineering from Concordia University, Montreal, QC, Canada, in 2019. From 2010 to 2012, he was a Lecturer with the Communication Department, Faculty of Engineering, Baniwaleed University. He was a Teaching Assistant with the Department of communication Engineering, College of Electronic Technology, Baniwaleed. His current research interests include analysis and antenna design, high gain millimeter-wave antennas, dielectric resonator antennas, and frequency selective surface (FSS).

ABDEL-RAZIK SEBAK (Life Fellow, IEEE) received the B.Sc. degree (Hons.) in electrical engineering from Cairo University, Cairo, Egypt, in 1976, the B.Sc. degree in applied mathematics from Ein Shams University, Cairo, in 1978, and the M.Eng. and Ph.D. degrees in electrical engineering from the University of Manitoba, Winnipeg, MB, Canada, in 1982 and 1984, respectively. From 1984 to 1986, he was with Canadian Marconi Company, where he was involved in the design of microstrip phased array antennas. From 1987 to 2002, he was a Professor with the Department of Electronics and Communication Engineering, University of Manitoba. He is currently a Professor with the Department of Electrical and Computer Engineering, Concordia University, Montreal, QC, Canada. His research interests include phased array antennas, millimeter-wave antennas and imaging, computational electromagnetics, and interaction of EM waves with engineered materials and bioelectromagnetics. He is a member of the Canadian National Committee of International Union of Radio Science Commission B. He was a recipient of the 2000 and 1992 University of Manitoba Merit Award for outstanding Teaching and Research, the 1994 Rh Award for Outstanding Contributions to Scholarship and Research, and the 1996 Faculty of Engineering Superior. He has served as the Chair of the IEEE Canada Awards and Recognition Committee, from 2002 to 2004, and the Technical Program Chair of the 2002 IEEE CCECE Conference and the 2006 URSIANTEM Symposium. He is also the Technical Program Co-Chair of the 2015 IEEE ICUWB Conference.